Efficient coupling of Sec23-Sec24 to Sec13-Sec31 drives COPII-dependent collagen secretion and is essential for normal craniofacial development

Anna K. Townley[1], Yi Feng[2], Katy Schmidt[1], Deborah A. Carter[2], Robert Porter[3], Paul Verkade[1,2] and David J. Stephens[1,*]

[1]Cell Biology Laboratories, Department of Biochemistry and [2] Department of Physiology and Pharmacology, and Wolfson Bioimaging Facility, University of Bristol School of Medical Sciences, University Walk, Bristol BS8 1TD, UK
[3]School of Biological Sciences, University of Bristol, Woodland Road, Bristol BS8 1UG, UK
*Author for correspondence (e-mail: david.stephens@bristol.ac.uk)

Accepted 25 June 2008
Journal of Cell Science 121, 3025-3034 Published by The Company of Biologists 2008
doi:10.1242/jcs.031070

Summary

The COPII coat assembles on endoplasmic reticulum membranes to coordinate the collection of secretory cargo with the formation of transport vesicles. During COPII assembly, Sar1 deforms the membrane and recruits the Sec23-Sec24 complex (Sec23/24), which is the primary cargo-binding adaptor for the system, and Sec13-Sec31 (Sec13/31), which provides a structural outer layer for vesicle formation. Here we show that Sec13 depletion results in concomitant loss of Sec31 and juxtanuclear clustering of pre-budding complexes containing Sec23/24 and cargo. Electron microscopy reveals the presence of curved coated profiles on distended endoplasmic reticulum, indicating that Sec13/31 is not required for the generation or maintenance of the curvature. Surprisingly, export of tsO45-G-YFP, a marker of secretory cargo, is unaffected by Sec13/31 depletion; by contrast, secretion of collagen from primary fibroblasts is strongly inhibited. Suppression of Sec13 expression in zebrafish causes defects in proteoglycan deposition and skeletal abnormalities that are grossly similar to the craniofacial abnormalities of *crusher* mutant zebrafish and patients with cranio-lenticulo-sutural dysplasia. We conclude that efficient coupling of the inner (Sec23/24) and outer (Sec13/31) layers of the COPII coat is required to drive the export of collagen from the endoplasmic reticulum, and that highly efficient COPII assembly is essential for normal craniofacial development during embryogenesis.

Supplementary material available online at
http://jcs.biologists.org/cgi/content/full/121/18/3025/DC1

Key words: COPII, Membrane traffic, Secretion, Vesicle formation

Introduction

COPII-dependent budding from the endoplasmic reticulum (ER) is required for the efficient export of secretory proteins (Barlowe et al., 1994). COPII assembly is initiated by a transmembrane protein within the ER membrane, Sec12, which catalyzes guanine nucleotide exchange on the small GTPase Sar1. Sar1-GTP subsequently recruits a heterodimeric complex of Sec23 and Sec24 (Sec23/24), which is responsible for the capture of cargo proteins into nascent buds. COPII assembly proceeds through recruitment of Sec13 and Sec31 (Sec13/31), which form a structural cage around the budding vesicle. In elegant FRET assays of COPII assembly and cargo capture, Sato and Nakano (Sato and Nakano, 2005) have shown that Sec23/24 can stably assemble onto membranes in the presence of cargo through direct protein-protein interactions; this maintains Sec23/24 on the membrane during the Sar1-GTP cycle. In other in vitro data, Sar1 in its GTP-bound form has been directly implicated in the generation of membrane curvature through integration of its N-terminal amphipathic helix (Bielli et al., 2005; Lee et al., 2005). Sec13/31 can self-assemble into cage-like structures that could conceivably provide the driving force for membrane deformation (Stagg et al., 2006). Indeed, widely proposed models of Sec13/31 function (Mancias and Goldberg, 2005), including our own (Watson and Stephens, 2005), typically implicate Sec13/31 in the stabilization of the membrane association of Sec23/24 and accumulation of cargo, in the initiation and propagation of membrane curvature, and in the final scission event. Recent data have shown that, at least in vitro, Sec13/31 is not required for the formation of the pre-budding complex containing Sar1, Sec23/24 and associated cargo (Sato and Nakano, 2005). Although it is clear that the pre-budding complex of Sar1-Sec23/24 and cargo can form in vitro, the precise role of Sec13/31 in stabilizing the recruitment of cargo and in the deformation of the membrane has not been explored in intact cells.

In *Saccharomyces cerevisiae* and humans, good evidence exists that Sec13 is required for the generation of transport vesicles from the ER (Salama et al., 1993; Tang et al., 1997). Sec31 is similarly required for ER-to-Golgi transport in many assays (Salama et al., 1997; Tang et al., 2000). However, in yeast, Hsp150 was shown to be secreted in *SEC13-1* mutant cells (Fatal et al., 2002). A series of 'bypass Sec13' mutants have been isolated (Elrod-Erickson and Kaiser, 1996). These gene products negatively regulate COPII vesicle formation and are required for proper discrimination of cargo from ER residents in budding assays. These data suggest that, in some cases in which Sec13-function is impaired but probably not abolished (e.g. through temperature-sensitive mutation), ER export of some cargo can continue. We have used siRNA-mediated suppression of Sec13 and a combination of single-cell imaging, fluorescence photobleaching, electron microscopy (EM) and zebrafish genetics to

define the role of Sec13/31 in vivo. Although our approaches do not lead to a complete loss of Sec13 from cells, we show that, in cells possessing less than 10% of their normal level of Sec13 expression, the ER is distended and decorated with large, open-necked budding profiles, but transport of small transmembrane cargo is normal; by contrast, collagen secretion is markedly inhibited by Sec13 depletion. Suppression of Sec13 expression in zebrafish results in defective proteoglycan secretion and in defects in craniofacial development, mimicking genetic loss of Sec23A function. It is important to note that, in both experimental systems, the expression of Sec13/31 is depleted but not abolished. These data and other recently published work (Bi et al., 2007; Fromme et al., 2007) suggest key roles for Sec13/31 in the completion of COPII-mediated budding through stimulation of the GTPase activity of Sar1. Together, these data show that sufficient levels of Sec13/31 and efficient assembly of the full COPII coat are required for effective secretion of selective components, notably of the extracellular matrix, and that this has direct implications for craniofacial development.

Results

Efficient suppression of Sec13 expression

Depletion of Sec13 or Sec31 was achieved using siRNA duplexes transiently transfected into HeLa cells. Fig. 1 shows the efficacy of depletion by immunoblotting. Lamin-A/C was used as a targeted siRNA control with α-tubulin as loading controls. Notably, we observed a concomitant decrease in Sec31 expression upon Sec13 depletion (Fig. 1A). We were also able to effectively suppress expression of Sec31A from cells (Fig. 1B). We were unable to achieve a high level of suppression of expression of the second human Sec31 homologue, Sec31B (Fig. 1C), and this was further complicated by the detection of multiple bands by the Sec31B-specific antibody, which could reflect splice forms, degradation products of Sec31B (Stankewich et al., 2006) or non-specific detection. Loss of Sec31A from cells correlated with efficiency of Sec13 silencing (Fig. 1D), with the most-effective depletion of Sec13 and concomitant loss of Sec31A from cells occurring 72 hours after siRNA transfection. By contrast, loss of Sec31A alone (with limited suppression of Sec31B expression) did not cause concomitant loss of Sec13 (supplementary material Fig. S1). Unlike with other COPII components, there is only one Sec13 isoform in humans and, thus, coupled with concomitant loss of Sec31A upon Sec13 suppression, we anticipated that efficient suppression of Sec13 alone is likely to have key implications for COPII function.

Formation and clustering of pre-budding complexes following Sec13 suppression

Following depletion of Sec13/31 expression, we determined the intracellular localization of markers of the ER-Golgi boundary in cells (Fig. 2). Depletion of Sec13 causes a clear reduction of Sec31A-positive labelling (Fig. 2A), consistent with the results of the immunoblotting experiments shown in Fig. 1. Furthermore, Sec13 depletion caused a relocalization of COPII (Sec24C and Sec16) and cargo (ERGIC-53) to the juxtanuclear region, which is very reminiscent of the effects of expression or microinjection of a GTP-restricted mutant of Sar1 (e.g. Stephens and Pepperkok, 2004). In addition, the Golgi (GM130-labelling) becomes more compact in these cells yet retains its characteristic juxtanuclear localization. Similar (although not so dramatic) effects were seen following depletion of Sec31A and Sec31B together (Fig. 2B; using the most effective siRNA duplexes against each isoform, Sec31A-2 and Sec31B-2, see Fig. 1); we attribute the lesser severity of the phenotype to the less effective depletion of these proteins. Images in each column of Fig. 2A were taken at the same imaging settings and therefore reveal this dramatic accumulation, particularly that of the otherwise more diffuse ERGIC-53 labelling, in the juxtanuclear region. This accumulation of COPII and ERGIC-53 is not due to an upregulation of protein synthesis, as was determined by immunoblotting (Fig. 2C). Fig. 2D shows the localization of ERGIC-53 at a lower exposure in Sec13-suppressed cells; here, one can clearly see the juxtanuclear accumulation of both Sec16 and ERGIC-53 following Sec13 suppression compared with lamin-A/C-suppressed controls. During the early secretory pathway, COPII function is closely coupled to COPI (Scales et al., 1997). Immunolabelling shows the classical Golgi and peripheral punctate labelling seen for COPI (Fig. 2E, here localizing the β-COP subunit), and the global loss of COPI from membranes in Sec13-suppressed cells with some remaining localization to both Golgi-like structures and peripheral punctae. Effective suppression is evidenced by loss of Sec31A labelling. Despite this clear perturbation of the early secretory pathway in Sec13-suppressed cells, localization of human β1,4 galactosyltransferase I (GalT, a marker of the trans-Golgi) was unchanged compared with lamin-A/C-suppressed controls, retaining its characteristic juxtanuclear localization (data not shown).

To investigate the nature of these juxtanuclear accumulations of COPII and cargo in more detail, we performed fluorescence

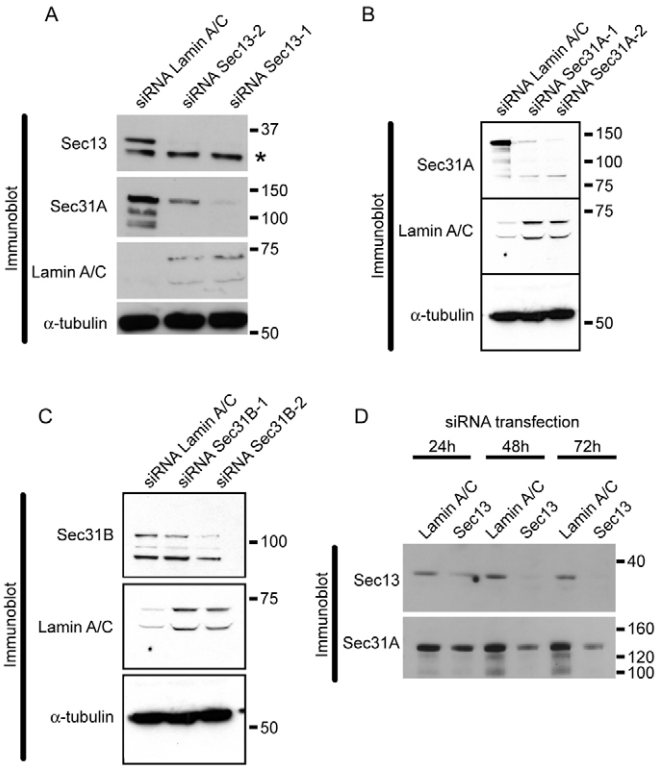

Fig. 1. Depletion of Sec13 expression by siRNA causes concomitant loss of Sec31. HeLa cells were transfected with two independent siRNA duplexes (-1 and -2) targeting either (A) *Sec13*, (B) *Sec31A* or (C) *Sec31B*; 72 hours later, cells were lysed and immunoblotted as indicated. (D) A time course showing concomitant loss of Sec13 and Sec31A at 24, 48 and 72 hours. Lamin A/C was used as a control in all experiments and α-tubulin is included as a loading control. Molecular-mass markers are shown in kDa. The asterisk in A marks a non-specific band.

recovery after photobleaching (FRAP) to determine whether COPII could continue to cycle on and off these structures [as would be predicted from the work of Sato and Nakano (Sato and Nakano, 2005)]. FRAP experiments (Fig. 3) showed a statistically significant increase (P=0.0072) in the half life of recovery of YFP-Sec23A in Sec13-depleted cells compared with controls (Fig. 3A). This indicates an increased residency time on the ER membrane. The immobile fraction of YFP-Sec23A at ER exit sites (ERES) shows a statistically significant increase (P=0.0097) following depletion of Sec13 compared with controls (Fig. 3B), indicating that a larger fraction of the protein is stably associated with ERES membranes at any one time. Furthermore, GFP–ERGIC-53 (Ben-Tekaya et al., 2005) showed rapid recovery into photobleached areas, indicating cargo entry into and exit from these structures, consistent with continuity with the underlying ER membranes (not shown).

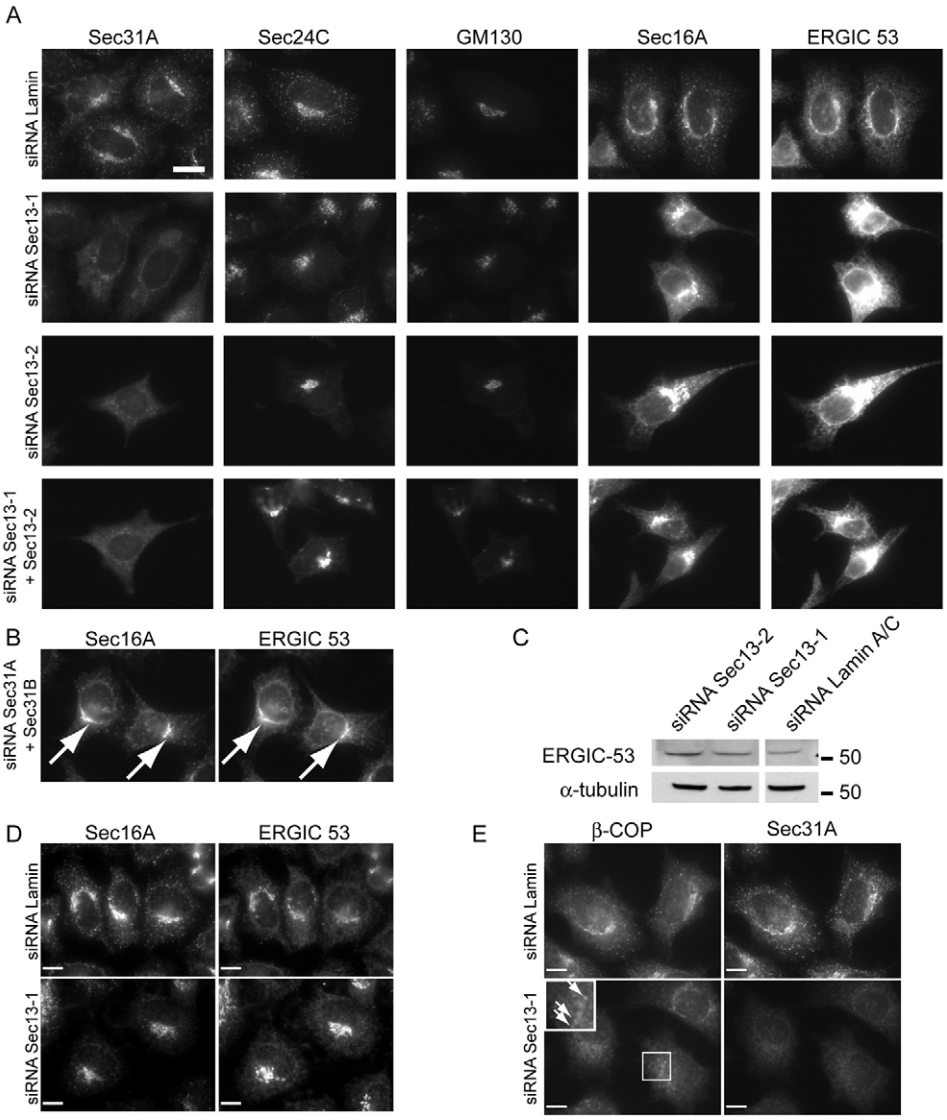

Fig. 2. Depletion of Sec13 causes a loss of peripheral ERES labelling, and an accumulation of COPII and cargo in the juxtanuclear region of cells. (A) Cells depleted of Sec13 for 72 hours using one or both of the siRNA duplexes (-1 or -2) were fixed and immunolabelled for Sec31A, Sec24C, GM130, Sec16 or ERGIC-53 as indicated. (B) Cells transfected with siRNA duplexes targeting both *Sec31A* and *Sec31B* were immunolabelled for Sec16 and ERGIC-53. Note the juxtanuclear accumulation of COPII (Sec16) and cargo (ERGIC-53) in both cases (arrows). (C) Lysates of cells depleted of Sec13 were immunoblotted with antibodies specific for ERGIC-53 and α-tubulin. Molecular-mass markers are shown in kDa. (D) Localization of Sec16A and ERGIC-53 at sub-saturating pixel intensities in lamin-A/C- or Sec13-suppressed cells. (E) Suppression of Sec13 expression causes a reduction in COPI labelling of both Golgi and peripheral punctae compared with lamin-A/C-suppressed controls. Sec31A labelling is used to show effective suppression of Sec13/31 expression. Scale bars: 10 μm.

Transport of tsO45-G-YFP is unperturbed by Sec13 depletion

To further define the requirement for Sec13 in ER export, we carried out a transport assay in cells expressing the temperature-sensitive glycoprotein tsO45-G-YFP (Gallione and Rose, 1985; Keller et al., 2001). Sec13 is required for ER export in many systems but, much to our surprise, depletion of Sec13 did not inhibit the transport of tsO45-G-YFP through the secretory pathway (Fig. 4). In these assays, cells depleted of Sec13 for 48 hours were infected at 39.5°C with an adenovirus expressing tsO45-G-YFP (Keller et al., 2001); under these conditions, tsO45-G-YFP is retained in the ER. After a further 16 hours, cells were shifted to 32°C to allow export of tsO45-G-YFP. Fluorescence microscopy showed that tsO45-G-YFP was equally delivered through the secretory pathway at 32°C in lamin-A/C-depleted cells and Sec13-depleted cells (Fig. 4A). Also evident in Fig. 4A (total tsO45-G-YFP) is the juxtanuclear condensation of labelling following Sec13 depletion, as would be predicted from the data in Fig. 2. Arrival of tsO45-G-YFP at the plasma membrane (shown by immunolabelling with an antibody directed against the extracellular epitope in non-permeabilized cells, Fig. 4A, lower panels) is indistinguishable between lamin-A/C- and Sec13-suppressed cells. Quantification of the delivery of tsO45-G-YFP to the plasma membrane showed no significant difference in Sec13-suppressed cells compared with lamin-A/C-suppressed controls (Fig. 4B). Knockdown efficiency was confirmed by Sec31A immunolabelling (data not shown). In order to define any subtle kinetic differences in ER-to-Golgi transport, we measured the delivery of the protein to the Golgi by monitoring acquisition of EndoH resistance by tsO45-G-YFP; this was similarly unaffected by Sec13 depletion (Fig. 4D) compared with controls (Fig. 4C) (one representative example is shown). This provides a more sensitive detection of ER-to-Golgi transport than delivery to the plasma membrane; despite a very strong suppression of Sec13 expression in these experiments, no significant differences were seen in the delivery of tsO45-G-YFP to the Golgi. Visual inspection of time-lapse sequences also showed no differences in delivery of tsO45-G-YFP to the juxtanuclear region (data not shown). Given the essential nature

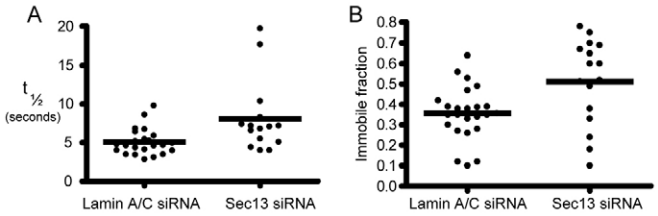

Fig. 3. Depletion of Sec13 causes an increase in the half life and immobile fraction of Sec23/24 at ERES. (A) Half life of recovery of YFP-Sec23A during photobleaching shows a statistically significant increase following depletion of Sec13 (P=0.0072; n=45 ERES from three independent experiments). (B) The immobile fraction of YFP-Sec23A at ERES shows a statistically significant increase following depletion of Sec13 (P=0.0097; n=45 ERES from three independent experiments).

of Sec13/31 for cell function, we were very surprised to find that transport of tsO45-G-YFP from the ER to Golgi and on to the plasma membrane was not significantly slowed in cells depleted of Sec13 compared with wild type. A huge array of evidence argues against Sec13/31 being dispensable for function in COPII vesicle biogenesis (e.g. Pryer et al., 1993; Salama et al., 1997; Tang et al., 1997; Matsuoka et al., 1998), and we interpret our data as indicating that the small quantity of Sec13/31 remaining following siRNA suppression is sufficient for efficient transport of tsO45-G-YFP. Our data suggest that the quantity of Sec13/31 normally expressed within HeLa cells is not required for all ER export. Because our experiments only provide a reduction in Sec13/31 expression and do not entirely abolish it, our data are consistent with an essential role for small amounts of Sec13/31 in ER export.

Sec13 suppression results in distended ER and in the accumulation of coated budding profiles

In order to examine the ultrastructure of ER and associated buds in Sec13-depleted cells, we performed EM of high-pressure frozen and freeze-substituted samples (Fig. 5). In control cells (Fig. 5A), we routinely observed budding profiles from ribosome-free areas of ER in close proximity to Golgi membranes (Fig. 5A, arrowhead). Following Sec13 depletion, distended ER was evident throughout cells, and frequently in the vicinity of Golgi membranes (Fig. 5B and enlarged in Fig. 5C). This distended region was largely ribosome-free, which is consistent with the enlargement of transitional ER and perhaps reflects the increased fluorescence intensity in this region seen in Fig. 2. Distended ER was also evident at peripheral sites within the cell, away from the Golgi (data not shown). These ER structures were also decorated with budding profiles that were reminiscent of COPII buds at transitional ER. Budding profiles in close proximity to Golgi membranes could alternatively be COPI coated. These buds were larger than the vesicular profiles seen in control cells (Fig. 5A, arrow). In addition to these large structures, we also observed more-typical coated vesicle profiles, which were in association with presumed ERES (Fig. 5B, arrows). Budding of coated vesicles from the Golgi appeared to be unaffected and, from inspection of multiple images, the Golgi did not appear to be significantly distended following Sec13 suppression. These data suggest that at least a subset of COPII-dependent budding from the ER is perturbed upon Sec13 depletion.

Collagen secretion and deposition is inhibited by Sec13 suppression

These vesicle bud profiles and distended ER are highly reminiscent of those seen in patient fibroblasts from sufferers of cranio-lenticulo-sutural dysplasia (CLSD; OMIM #607812) (Boyadjiev et al., 2006; Fromme et al., 2007). One key feature of this disorder is the accumulation of collagen in fibroblasts. We therefore examined the effect of suppressing Sec13 expression on collagen secretion from human primary dermal fibroblasts. Fig. 6A shows that control (lamin-A/C suppressed) cells show strong deposition of collagen, as shown by labelling for the C-terminal telopeptide (using antibody

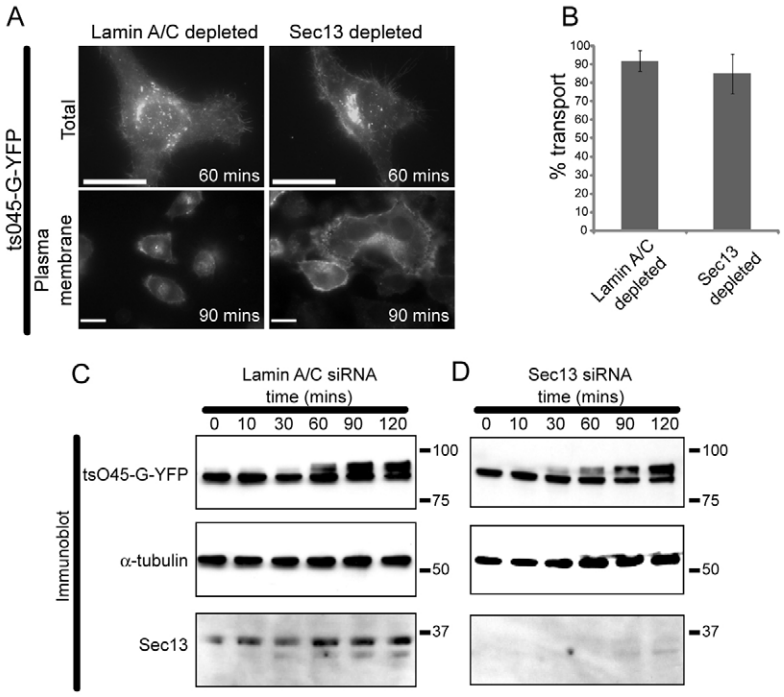

Fig. 4. Secretory transport of tsO45-G-YFP is not significantly inhibited following Sec13 depletion. Cells depleted of Sec13 or lamin A/C were infected with an adenovirus expressing tsO45-G-YFP followed by incubation at the restrictive temperature of 39.5°C for 18 hours. (A) Transport of tsO45-G-YFP through the secretory pathway in cells transfected with either lamin-A/C or *Sec13* siRNA. Upper panels: YFP (total tsO45-G) fluorescence 60 minutes after the shift to 32°C shows indistinguishable Golgi localization and plasma-membrane delivery in either experiment; note the enhanced juxtanuclear clustering of the Golgi in Sec13-suppressed cells. Lower panels: shows only plasma-membrane-localized tsO45-G-YFP 90 minutes after the shift to 32°C. Scale bars: 20 μm. (B) Quantification of arrival of tsO45-G-YFP at the plasma membrane (monitored by immunolabelling paraformaldehyde-fixed but non-permeabilized cells with an antibody against an extracellular epitope); error bars show standard deviation (n=100 cells from three independent experiments). (C,D) Arrival of protein at the Golgi following release of cargo from the ER at 32°C for the times indicated was determined by monitoring acquisition of EndoH resistance and immunoblotting for YFP. Samples were also immunoblotted to confirm the efficacy of Sec13 depletion and α-tubulin was included as a loading control. Molecular-mass markers are shown in kDa.

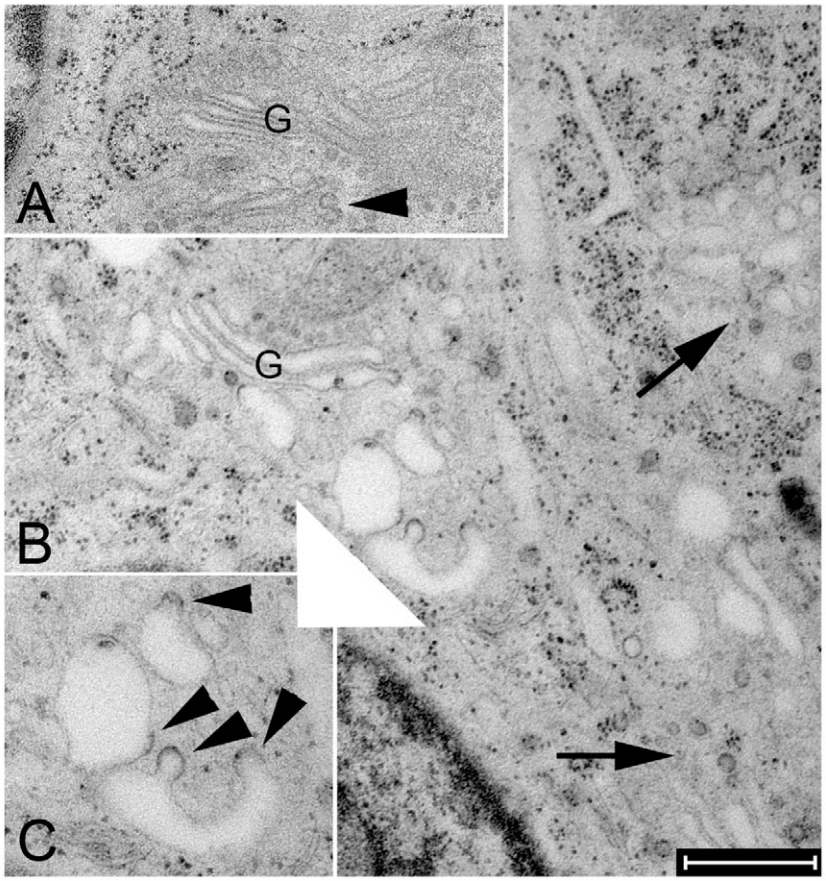

Fig. 5. Ultrastructure of ER bud sites in Sec13-suppressed cells. Electron micrographs of high-pressure-frozen and freeze-substituted HeLa cells. (A) In control (lamin-A/C depleted) cells, small 50 nm vesicles are in close proximity to the Golgi apparatus (G). These vesicles are presumptive ER-to-Golgi transport vesicles but could potentially be either COPI- or COPII-coated. Occasionally, a coated (COPII) budding profile can be observed emanating from the ER (arrowhead). (B,C) In Sec13-depleted cells, the small 50 nm vesicles can still be observed (arrows) but, in addition, dilated ER with several budding profiles can frequently be seen (B, inset in C shows magnification of indicated area, large white arrowhead). These budding profiles (arrowheads in C) appear to be in different states of fission and contain an electron-dense coat. Scale bar: 500 nm (A,B), 350 nm (C).

LF-67, arrowheads in Fig. 6A indicate robust deposition of extracellular collagen fibrils); these cells also show relatively uniform labelling for Sec31A. By contrast, cells depleted of Sec13 show much less deposition of extracellular collagen fibrils (compared with lamin-A/C-suppressed cells) and loss of Sec31A labelling (consistent with our data from HeLa cells). Semi-automated image analysis was used to quantify these data. Thresholding images to detect only high pixel intensities allowed selective detection of collagen fibrils, which were then counted by measuring their skeletal length in large-format montage images of multiple fields of view acquired using an automated X-Y scanning stage (supplementary material Fig. S2). Further examination of intracellular procollagen using an antibody directed against the N-terminal propeptide of type I procollagen (LF-39) showed clear accumulation of unprocessed procollagen in cells depleted of Sec13/31 (supplementary material Fig. S2B, asterisks). These data revealed a >threefold loss of fibrillar-collagen deposition in Sec13-suppressed cells compared with lamin-A/C-suppressed controls (Fig. 6B). Immunoblotting confirmed effective suppression of Sec13 expression and concomitant loss of Sec31A from these cells (Fig. 6C). Multiple species of Sec31 were seen in primary fibroblasts, probably owing to the presence of multiple splice forms and/or post-translationally modified forms of the protein (Tang et al., 2000); all forms were suppressed by *Sec31A* siRNA transfection. Furthermore, the distribution of GalT in Sec13-suppressed fibroblasts was indistinguishable from that of control cells (data not shown). Thus, suppression of Sec13 expression reduces the secretion and deposition of collagen fibrils without significantly affecting the secretion of tsO45-G-YFP or the accumulation of GalT in the Golgi. These data reflect observations made in patient fibroblasts from CLSD cases (Fromme et al., 2007).

Zebrafish Sec13 morphants show defects in craniofacial development

Many phenotypic aspects of CLSD are recapitulated in *crusher* mutant zebrafish (Lang et al., 2006); both CLSD and *crusher* are caused by a mutation in *Sec23A* (Boyadjiev et al., 2006; Lang et al., 2006). To examine the role of Sec13/31 in vivo, we used morpholino oligonucleotide-based suppression of *Sec13* expression in embryos of the zebrafish *Danio rerio*. Two non-overlapping translation-blocking morpholinos were used for these experiments. Sec13 morphants were viable [at least until 5 days post fertilization (dpf)] but were smaller overall, had smaller heads and eyes, and showed pigmentation defects (Fig. 7A). Fig. 7B shows that, at 5 dpf, Sec13 morphant embryos have defects in craniofacial development and the pectoral fins are kinked (arrows in wild-type, arrowheads in Sec13 morphants). This phenotype shows some similarity to the Group-II classification (mutations affecting cartilage differentiation and morphogenesis) of Neuhauss and colleagues (Neuhauss et al., 1996), which includes the *crusher* mutant. Alcian-blue staining (which primarily stains proteoglycans of extracellular-matrix components) to reveal the skeleton shows that, at 4 dpf, there is a noticeable absence of cartilage formation at the front of the head (e.g. Meckel's cartilage; Fig. 7C, mc) in Sec13 morphants. The defect is more pronounced at 5 dpf, which reveals extensive disorganization of structure within the neurocranium and defects in the pectoral fin, which is kinked and often malformed. Additional images obtained from experiments using alternative morpholino oligonucleotides are shown in supplementary material Fig. S3. Scanning electron microscopy (Fig. 7D, showing dorsal, lateral and ventral views) shows clearly the defects in craniofacial (Fig. 7D, arrowhead) and pectoral-fin (Fig. 7D, arrow) development. Notably, a clear defect in eye morphogenesis is also evident from these images; we are currently investigating this further. Immunoblotting of lysates of dechorionated embryos confirms the reduction in Sec13 expression (Fig. 7E). Furthermore, the embryos show a concomitant loss of Sec31A (Fig. 7E), as we observed for HeLa cells (Fig. 1). Although these blots show that suppression of expression of Sec13 in zebrafish embryos is less effective than in tissue-culture cells, our

data show clearly that the deposition of proteoglycan is impaired and that this correlates with clear defects in craniofacial development.

Discussion

Our data provide key information regarding Sec13/31 function in intact cells and during embryonic development. We found that Sec13 is required to maintain the structural stability of Sec31. Depletion of Sec13/31 causes a clustering of pre-budding complexes containing Sec16, Sec23/24 and cargo in a juxtanuclear area, which is highly reminiscent of the phenotype following expression of a GTP-restricted form of Sar1. The remaining COPII-coat associated with these pre-budding complexes is stabilized in Sec13-depleted cells. Sec13/31 suppression causes distension of the ER and accumulation of budding profiles on the ER membrane. Collagen secretion is defective but transport of smaller cargo is unperturbed. Finally, suppression of Sec13 in zebrafish causes defects in proteoglycan secretion and craniofacial-development defects.

The finding that Sec13 is required to maintain the stability of Sec31 is entirely consistent with the X-ray crystallographic structure of the Sec13/31 complex, in which part of Sec31 is seen to form one blade of the Sec13 WD40 propeller structure (Fath et al., 2007). In line with data obtained from in vitro reconstitution experiments (Matsuoka et al., 1998), we found that >90% depletion of Sec13/31 expression does not perturb the association of Sec23/24 or Sec16 with the membrane. Thus, pre-budding complexes are able to form, recruit cargo and accumulate in the juxtanuclear area. Recent kinetic data from in vitro binding experiments show that the association of Sec23/24 with cargo on membranes can be maintained despite ongoing GTP hydrolysis by Sar1 (Sato and Nakano, 2005). The presence of Sec23/24 on the membrane can be maintained by interactions with cargo proteins (Sato and Nakano, 2005) and the continual GTP loading of Sar1 by Sec12 (Futai et al., 2004). Indeed, the rate of GTPase stimulation by Sec23 is balanced by the rate of GTP loading by Sar1 such that a continual supply of Sar1-GTP is maintained. The binding and further stimulation of GTP hydrolysis by Sec13/31 results in a net loss of active Sar1 from the membrane (Antonny et al., 2001). Our FRAP experiments provide support for this model in living cells. We conclude that it is the recruitment of Sec13/31 that is required to stimulate Sar1 GTPase activity in vivo, either by acting on the conformation of the Sec23/24 complex in association with Sar1, or (as indicated by other recent data) through a direct effect on Sar1 itself (Fath et al., 2007).

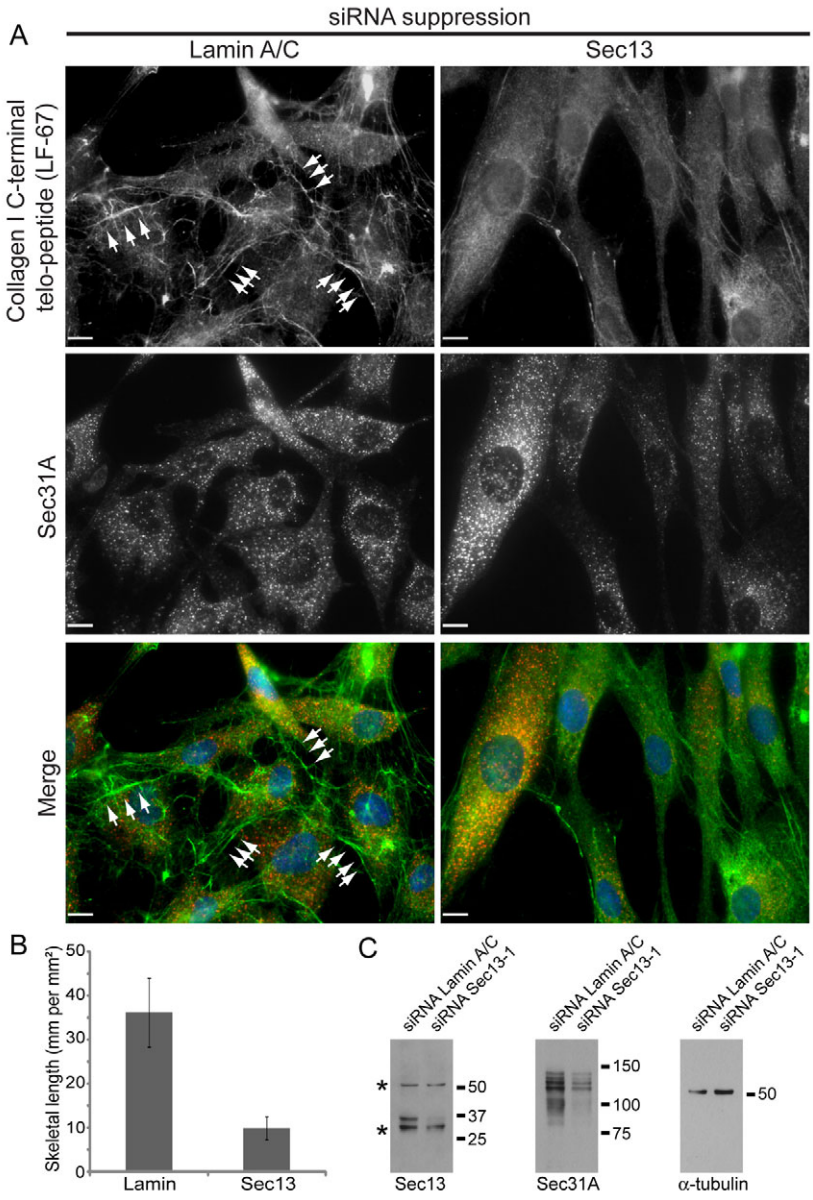

Fig. 6. Suppression of Sec13 in primary human fibroblasts results in defective collagen secretion and deposition. Primary human dermal fibroblasts were transfected with siRNA duplexes to suppress Sec13 expression for 72 hours. Cells were then processed for immunofluorescence using antibodies to detect type-I collagen and Sec31A. (A) Cells were labelled with antibodies to detect the C-terminal telopeptide of collagen I (LF-67) and Sec31A. Scale bars: 20 μm. (B) Quantification of collagen deposition from three independent experiments shows a significant reduction (P<0.001) in deposition of fibrillar collagen. Supplementary material Fig. S2 shows further detail and example images from this quantification. (C) Immunoblotting was used to verify suppression of Sec13 and concomitant loss of Sec31A in primary human dermal fibroblasts. Asterisks denote non-specific bands detected with the anti-Sec13 antibody; tubulin was included as a loading control. Molecular-mass markers are shown in kDa.

Our EM data indicate that suppression of Sec13/31 does not prevent either the generation or stabilization of membrane curvature. Thus, these properties probably lie in other COPII components, which could include Sec16, which, in concert with Sar1, can form large curved structures in cells (Watson et al., 2006), and/or Sec23/24, which is proposed to adopt a curved conformation (Bi et al., 2002). Curvature of the membrane can result from activation of Sar1 to its GTP-bound form, directing association of its amphipathic N-terminus with the membrane (Bielli et al., 2005; Lee et al., 2005). GTP hydrolysis by Sar1 could result in scission of the vesicle from the membrane through perturbation of a bilayer structure (Bielli et al., 2005; Lee et al., 2005). In Sec13-depleted cells, the loss of Sec13/31 GAP activity could limit the potential for membrane scission, resulting in a decrease in carrier formation.

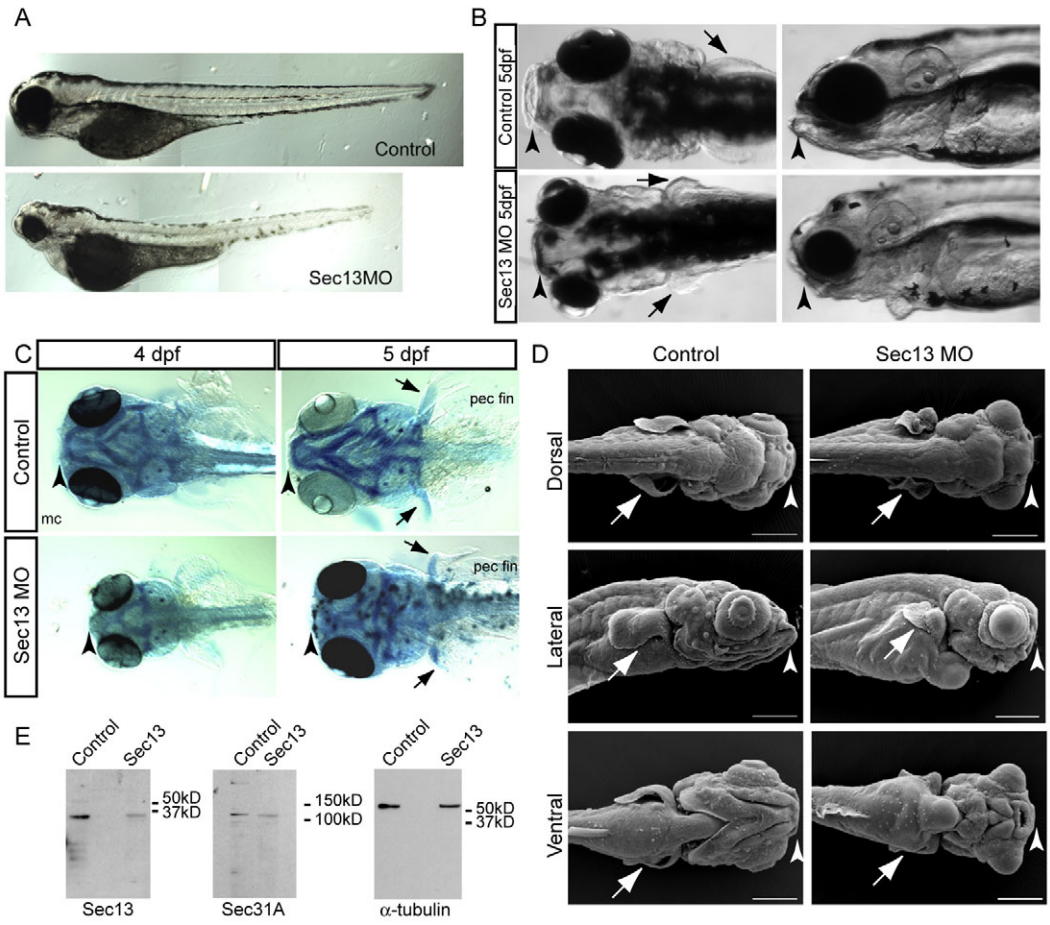

Fig. 7. Suppression of Sec13 expression in *D. rerio* results in a phenotype similar to that of *crusher* mutant embryos. (A) Control and Sec13 morphant (using morpholino oligonucleotide MO1) zebrafish embryos at 5 dpf were photographed following paraformaldehyde fixation. (B) Live embryos were photographed at higher magnification to visualize craniofacial features (from experiments using MO2). Arrows indicate the facial features and arrowheads the pectoral fins that are present in controls but missing or dysmorphic in Sec13 morphants; note the absence of extension of the head beyond the eyes and kinked pectoral fin in Sec13 morphants. (C) Alcian-blue staining of fixed embryos at 4 and 5 dpf (following microinjection of MO1) shows defective deposition of proteoglycans and lack of formation of cartilage in multiple areas of the head. mc, Meckel's cartilage; pec fin, pectoral fin. Arrows indicate facial features and arrowheads the pectoral fins in controls that are missing or dysmorphic in Sec13 morphants (arrowheads). (D) Scanning electron micrographs showing the dorsal, lateral and ventral views of control and Sec13 morphant 5-dpf zebrafish embryos. Note the perturbation of development of the frontal region of the head (arrowhead), the pectoral fins (arrows) and the eyes in Sec13 morphants. Scale bars: 0.2 mm. (E) Immunoblotting of lysates from dechorionated control or Sec13 morphant embryos confirms suppression of Sec13 expression and concomitant loss of Sec31A. Immunoblotting of these lysates for α-tubulin is included as a loading control. Molecular-mass markers are shown in kDa.

It is also possible that Sec13/31-stimulated Sar1 GTPase activity is required for faithful incorporation of certain cargoes. Functions have been shown for Sar1 GTPase activity in the fidelity of cargo sorting into COPII vesicles (Sato and Nakano, 2004), and differing requirements for Sar1-GTPase activity in terms of cargo incorporation in to pre-budding complexes have been found (Stephens and Pepperkok, 2004). The defined coat in our EM images probably reflects accumulation of Sar1-Sec23/24 complexes on the membrane; this is largely absent in images from patient fibroblasts (Fromme et al., 2007), which could either reflect a difference in preparation method or could suggest that pre-budding complexes containing Sec23A-F382L are less stably associated with the ERES membrane than those containing wild-type Sec23A.

Defects in COPII-dependent budding have been identified as the underlying cause of CLSD (Boyadjiev et al., 2003; Boyadjiev et al., 2006; Lang et al., 2006; Fromme et al., 2007). CLSD results from a missense mutation in Sec23A [F382L (Boyadjiev et al., 2006)] that lies at the point of Sec23A that directly contacts Sec31 (Bi et al., 2007). This disease is characterized by facial dysmorphisms in humans (Boyadjiev et al., 2003) and is largely recapitulated by the *crusher* mutation in the zebrafish *D. rerio* (Neuhauss et al., 1996; Lang et al., 2006). The c*rusher* mutation is in fact a nonsense mutation in Sec23A (Lang et al., 2006), almost certainly resulting in non-functional protein. Both CLSD patients and *crusher* mutant zebrafish have defects in the export of both collagen and complex proteoglycans (Boyadjiev et al., 2006; Lang et al., 2006).

Recent data have suggested that the selective defect in CLSD patients and *crusher* zebrafish (i.e. that only certain cell types show a phenotypic defect and indeed that the patients and zebrafish are viable) is due to the presence of a second Sec23 isoform, Sec23B, in both humans (Boyadjiev et al., 2006; Fromme et al., 2007) and zebrafish (Lang et al., 2006). Low expression of Sec23B in calvarial osteoblasts (which are primarily responsible for the primary

ossification of the cranial suture) could mean that this isoform cannot compensate for defects in Sec23A and therefore these specific cell types show defects in secretion (Fromme et al., 2007). However, suppression of either Sec23A or Sec23B in zebrafish individually, or in combination, results in embryos that show craniofacial development defects (Lang et al., 2006). The efficacy of knockdown in these experiments was not shown, but these data show that neither Sec23A nor Sec23B is alone sufficient for proper craniofacial development in zebrafish. These data are consistent with those presented here if one considers that the expression of both Sec23A and Sec23B in calvarial osteoblasts together provide sufficient Sec23 to couple efficiently to the outer, Sec13/31, layer of the COPII coat. Our data reveal very similar phenotypes to those of CLSD patients and *crusher* zebrafish, and suggest that we are recapitulating the defect in the coupling of Sec13/31 to Sec23/24. Consequently, we conclude that, rather than a specific role for Sec23A (e.g. in the capture of specific cargo), it is the efficient and effective coupling of Sec23/24 to Sec13/31 that is the key requirement for craniofacial development.

Sec13 is expressed from the end of gastrulation onwards in zebrafish (Thisse et al., 2001) and, notably, during the first 48 hours of embryonic development, expression is highest in the notochord and during this time increases in the cleithrum, optic tectum and pectoral-fin musculature (Thisse et al., 2001), which correlates well with the developmental defects that we observe in Sec13 morphants (particularly those evident in scanning electron micrographs). Intriguingly, expression is also high in the otic vesicle and retina. Sec31 is also highly expressed in notochord, optic tectum, otic vesicle, cleithrum and fin (Thisse et al., 2001), again correlating well with our findings. This suggests an unusually high secretory load in these tissues at this stage of development, which requires highly efficient COPII function.

The dysmorphisms of the cranial structure that we observe in our Sec13 morphants is in fact most similar to that described for the *bulldog*, *Jekyll*, *mr hyde* and particularly *round* mutant zebrafish embryos (Neuhauss et al., 1996). *Jekyll* is caused by a mutation in UDP-glucose dehydrogenase that results in defective proteoglycan secretion (Walsh and Stainier, 2001). Taken together, our data and those of other laboratories (e.g. Fromme et al., 2007) suggest that Sec23A is not the sole component that is relevant to the secretion of collagen or proteoglycan, i.e. it is not the specific cargo selector involved. Rather, any defect in coupling of the inner and outer layers of the COPII coat appears to result in defects in secretion of large macromolecular cargo from the ER. Clearly, it will be of interest to determine whether any other craniofacial-development mutants in zebrafish or other clinical cases with craniofacial dysmorphisms are caused by mutation in Sec13, Sec31, other COPII subunits or indeed other components of the ER export machinery.

Surprisingly, despite a robust inhibition of collagen secretion and deposition, we did not observe any significant inhibition of transport of tsO45-G-YFP in cells depleted of Sec13/31, the Golgi remained largely unperturbed, and GalT remained localized to the Golgi cisternae, indicating that there was not a general defect in the transport of glycosylation enzymes to the Golgi. Other work strongly indicates that Sec13/31 is required to provide the final stimulus of Sar1 GTPase activity to trigger vesicle fission (Fath et al., 2007; Fromme et al., 2007). At first glance, this might be difficult to reconcile with our own work, in which we show that a near-complete loss of Sec13 has no significant effect on the trafficking of GalT or tsO45-G-YFP. However, we would argue that our data are in fact entirely consistent with this model, in particular if one invokes the intriguing possibility of selective recruitment of the remaining Sec13/31 to the bud neck to drive fission. Alternatively, it is possible that the remaining Sec31 is alone sufficient to stimulate Sar1 GTPase activity (because more Sec31 than Sec13 remains in each of our experiments, including following direct Sec31 suppression).

We hypothesize that normal expression levels of Sec13/31 are required to scaffold the formation of larger carriers emerging from the ER (such as those containing assembled, fibrillar collagen) but not for the secretion of smaller cargoes (tsO45-G-YFP or GalT). Scaffolding activity could require more-efficient coupling of Sec13/31 to Sec23/24 than does recruitment for a scission event. Thus, inefficient coupling of the inner and outer layers of the COPII coat through depletion of Sec13/31 from cells would result in a selective defect in secretion of large, macromolecular cargo. Our data therefore argue that efficient formation of the full COPII coat is of greater importance for collagen secretion than any direct role for Sec23A in, for example, cargo concentration. In addition to a defect in the secretion of fibrillar collagens and complex proteoglycans, this could include chylomicron retention diseases (OMIM #246700), in which the assembly of large apoB-containing chylomicrons is defective owing to mutation of Sar1B. Fromme and colleagues provide further evidence that differential coupling of Sar1 isoforms to Sec13/31 might underlie this disease (Fromme et al., 2007). In summary, our data indicate a selective requirement for non-limiting quantities of Sec13/31 in COPII-dependent export from the ER, and reveal a clear requirement for highly efficient COPII-coat assembly in craniofacial development.

Materials and Methods

Materials

All reagents were purchased from Sigma-Aldrich (Poole, UK) unless otherwise indicated. HeLa cells (ATCC CRL-2) were maintained in DMEM supplemented with 10% FCS (Invitrogen, Paisley, UK) and 1% glutamine. Primary human dermal fibroblasts were purchased from Cascade Biologics/Invitrogen and were cultured in Medium 106 supplemented with low-serum growth supplement. At 24 hours prior to the start of the experiments, cells were seeded onto either 22-mm coverslips or glass-bottom dishes (MatTek, Ashland, MA).

Monoclonal mouse anti-ERGIC-53 was from Alexis Biochemicals (Nottingham, UK), anti-GM130 was from BD Transduction Laboratories (Cambridge, UK), anti-tubulin from Neomarkers (Fremont, CA) and anti-GFP from Covance (Harrogate, UK). Polyclonal antibodies against Sec16A were from Bethyl Laboratories (Montgomery, TX), Sec13 antibodies were generous gifts from Wanjin Hong (IMCB, Singapore) and Beatriz Fontoura (Southwestern Medical Center, Dallas, TX), anti-lamin-A/C from Cell Signaling Technology (Hitchin, UK), mouse monoclonal anti-Sec31A was from BD Biosciences, and anti-β-COPI (maD) was from Sigma-Aldrich. Secondary antibodies were from Jackson ImmunoResearch Laboratories (PA). Anti-human GalT was from CellMab (Gothenburg, SE). Collagen-I antibodies [LF-39 directed against the human collagen α1 (I) amino-propeptide (Fisher et al., 1989) and LF-67 recognizing the human collagen α1 (I) carboxy-telopeptide (Bernstein et al., 1995)] were very generously provided by Larry Fisher (NIH, Bethesda, MD). Anti-Sec24C and -Sec31A antibodies were raised against synthetic peptides synthesized by Graham Bloomberg, University of Bristol and coupled to KLH before immunization into rabbits. Antibodies were affinity purified using peptide coupled to sulfolink resin (Pierce, Cramlington, UK) according to the manufacturer's protocols. Peptide sequences were as follows: Sec24C: MNVNQSVPPVPPFGQ(C); Sec31A: MKLKEVRTAMQAWS(C), in which C-terminal cysteines were added for coupling.

RNAi and transfection

siRNA duplexes against Sec13 were designed using the online algorithms of, and synthesized by, MWG-Biotech (London, UK). These sequences were: Sec13-1, 5′-GCACUCAUGUUACGAGGAA-3′; Sec13-2, 5′-GGAGGAGCAGAAGCUAGAA-3′; Sec31A-1, 5′-ACACAGGAGAGGUGUUAUA-3′; Sec31A-2_3′UTR, 5′-GCUUCUCUUCCACUCAAUA-3′; Sec31B-1, 5′-AGAUAUUGAUGGACU-CCUA-3′; and Sec31B-2, 5′-UUGGAGCCAUAUUAAGGAA-3′.

HeLa cells were transfected with siRNA duplexes using a calcium-phosphate method as previously described (Watson and Stephens, 2006). Primary human dermal fibroblasts were transfected using geneFECTOR (VennNova, FL) according to the

manufacturer's instructions. Times indicated for siRNA suppression (typically a total of 72 hours) refer to the time from the addition of siRNA duplexes.

Immunofluorescence

For immunofluorescence, cells were first washed with phosphate buffered saline (PBS) and then fixed with methanol at –20°C for 4 minutes, followed by blocking with PBS containing 3% bovine serum albumin (BSA) for 30 minutes. Primary antibodies were diluted to varying concentrations in PBS containing 3% BSA. Cells were incubated with primary antibodies for 1 hour at room temperature. They were subsequently washed with PBS and incubated with secondary antibodies, either Cy2 or Cy3, for 1 hour at room temperature. Cells were counterstained with DAPI and mounted onto slides using Mowiol. For collagen labelling, cells were fixed in paraformaldehyde for 20 minutes, permeabilized with 0.1% Triton X-100 for 5 minutes, blocked in 3% BSA/PBS and labelled with either LF-67 or LF-39 in combination with mouse monoclonal anti-Sec31A. Available Sec13 antibodies were not found to be suitable for immunofluorescence. Fixed cells were imaged on an Improvision 3DM system (Improvision, Coventry, UK) comprising an IX-81 microscope (Olympus Microscopes, London, UK), with ASI PZ-2000 XYZ stage (Applied Scientific Instruments, Eugene, OR) DG-4 illumination system (Sutter, Novato, CA, USA) with Brightline 'Pinkel' filter sets with single-band exciters and multi-band dichroic and emission filters (Semrock, Rochester, NY). Images were acquired using a Hamamatsu Orca-ER cooled CCD camera with Volocity version 4.2 (Improvision). Images were resized using Adobe Photoshop and montages were created using Adobe Illustrator CS (Adobe).

Fluorescence recovery after photobleaching

Cells were seeded onto live-cell dishes and siRNA transfected for 72 hours using oligofectamine (Invitrogen) as per the manufacturer's instructions. Cells were subsequently transfected with plasmid DNA using FuGENE, as per the manufacturer's instructions, 48 hours after siRNA transfection. Immediately before imaging, the media was aspirated from cells and replaced with imaging media (DMEM containing 30 mM HEPES). YFP-Sec23A (Stephens, 2003) and GFP-ERGIC-53 (Ben-Tekaya et al., 2005) have been previously described.

Cells were live imaged in a 37°C heated Perspex box (Life Imaging Services, Reinach, CH) on a Leica SP5 confocal imaging system (Leica Microsystems, Milton Keynes, UK) using 488 nm and 514 nm lines of an argon laser. A pinhole size of 3 Airy disk was used to take images using a Leica DMI 6000 inverted microscope. Cells were subjected to five pre-bleach frames, eight bleach frames using three lasers at 100% power and 140 post-bleach frames. Data was processed and statistical significance determined using GraphPad Prism (San Diego, CA).

Immunoblotting

Cells were grown on either 6- or 3-cm dishes until 80% confluent. Media was removed and cells were washed with ice-cold PBS before addition of ice-cold lysis buffer (50 mM Tris-HCl pH 7.4, 150 mM NaCl, 1 mM phenylmethyl sulphonylfluoride, 1% Triton X-100, 1× protease inhibitor cocktail). Cell scrapers were used to remove cells from the dish. Lysates were then centrifuged at 20,000 ***g*** at 4°C for 20 minutes to remove cell debris. Protein assays were carried out using a BCA protein assay kit (Pierce). Typically, between 10-20 μg of protein was loaded onto precast SDS-PAGE gels (Invitrogen). Rabbit anti-Sec13 (Wanjin Hong) and rabbit anti-Sec31A (described herein) were used for immunoblotting of lysates from both HeLa cells and fibroblasts.

Transport assay using EndoH

Cells were plated onto 3-cm dishes and siRNA transfected as above. At 48 hours after transfection, cells were infected with YFP-tsO45-G-virus for 2 hours at 37°C, 5% CO_2. The virus was then removed and fresh media added before shifting the cells to a 39.5°C, 5% CO_2 incubator for 16 hours. The dishes were placed in a 32°C water bath and, after each time point (0, 10, 20, 30, 60 and 90 minutes), cells were removed and washed with ice-cold PBS before addition of lysis buffer (50 mM Tris-HCl pH 7.4, 150 mM NaCl, 1 mM PMSF, 1% Triton X-100, 1× protease inhibitor cocktail). Cells were removed from the plates using a cell scraper and then transferred to a microcentrifuge tube and centrifuged at 20,000 ***g***, 4°C for 20 minutes to remove cell debris. The protein concentration was determined using a BCA protein assay kit (Pierce). Protein sample (10 μg) was heated at 95°C for 5 minutes in denaturing buffer (Invitrogen). Reaction buffer was added to each sample before adding 250 units of EndoH (NEB, Hitchin, UK) and incubating at 37°C for 16 hours. Following this, SDS sample buffer was added to the samples and heated at 95°C for 5 minutes. Subsequently, the samples were run on Bis-Tris polyacrylamide gels (Invitrogen) and probed with an anti-GFP antibody (Covance).

Transmission electron microscopy

Sec13- or lamin-A/C (control)-suppressed HeLa cells were grown on 1.5-mm sapphire discs. They were briefly rinsed in DMEM containing 30 mM HEPES, 10% FCS and 20% BSA. The latter two components were added to prevent freezing artefacts (McDonald et al., 2007). The sapphire disc was then placed in a 0.1-mm-deep membrane carrier and high-pressure frozen using the EMPACT2 with rapid-transfer system [Leica Microsystems (Verkade, 2008)]. The samples were subjected to a short-freeze-substitution protocol (Verkade, 2008). Briefly summarized, samples were placed in 1% OsO_4 and 0.1% uranyl acetate in ultra-pure acetone and left for 5 hours at –90°C. The temperature was slowly increased (5°C per hour) to 0°C and the samples were washed with ultra-pure acetone. They were gradually infiltrated with Epon and eventually embedded in moulds. The Epon was hardened overnight and ultrathin sections were counterstained and analyzed with a FEI Tecnai12 Biotwin (FEI, Eindhoven, The Netherlands) equipped with a bottom-mount 4K EAGLE CCD camera.

Danio rerio morpholino oligonucleotide microinjection and developmental analysis

Zebrafish (*D. rerio*) AB strain were raised and maintained as described previously (Westerfield, 1995). Two non-overlapping, translation-blocking morpholino oligonucleotides targeting *D. rerio Sec13* (BC153483.1) were designed and synthesized by GeneTools LLC (Philomath, OR). The sequences used were MO1: 5′-CACTGTGTTAATGACCGAAACCATG-3′ and MO2: 5′-TTTGCTTATAT-CCCTCAACAACCTC-3′. Morpholino knockdown of Sec13 protein level and expression levels of Sec31 and α-tubulin were confirmed by western blotting using antibodies against mammalian proteins that showed cross-reactivity to *D. rerio* orthologues. Embryos at 4 and 5 dpf were fixed in 4% PFA for 2 hours then mounted in 1% methylcellulose for photography. Alcian-blue staining of 4- and 5-dpf embryos was performed as described previously (Neuhauss et al., 1996); samples were mounted in 100% glycerol and all photographs were taken using Zeiss Axioplan2 5× or 10× lens (Zeiss, Welwyn Garden City, UK).

Scanning electron microscopy

For scanning electron microscopy, morpholino-injected zebrafish (5 dpf) were fixed in 4% PFA at 4°C, then post-fixed in 1% OsO_4 in dH_2O for 1 hour, dehydrated in graded ethanol, and critical-point dried (100% ethanol/carbondioxide). The specimens were sputter-coated with gold (Polaron Sputter Coater) and viewed on a Philips 501B emission scanning electron microscope.

We thank Harry Mellor, Jon Lane, Pete Watson, Pete Cullen and members of the Stephens lab for helpful discussions throughout this project, and Paul Martin for facilitating the work with zebrafish. We also thank Kai Simons, Patrick Keller, Hans-Peter Hauri, Larry Fisher, Wanjin Hong and Beatriz Fontoura for kind gifts of antibodies and plasmids. We thank the MRC for funding this work through a Senior Non-Clinical fellowship from (to D.J.S.), a research grant from the BBSRC, and the MRC, Wolfson Foundation for providing support to establish and develop the Wolfson Bioimaging Facility.

References

Antonny, B., Madden, D., Hamamoto, S., Orci, L. and Schekman, R. (2001). Dynamics of the COPII coat with GTP and stable analogues. *Nat. Cell Biol.* **3**, 531-537.

Barlowe, C., Orci, L., Yeung, T., Hosobuchi, M., Hamamoto, S., Salama, N., Rexach, M. F., Ravazzola, M., Amherdt, M. and Schekman, R. (1994). COPII: a membrane coat formed by Sec proteins that drive vesicle budding from the endoplasmic reticulum. *Cell* **77**, 895-907.

Ben-Tekaya, H., Miura, K., Pepperkok, R. and Hauri, H. P. (2005). Live imaging of bidirectional traffic from the ERGIC. *J. Cell Sci.* **118**, 357-367.

Bernstein, E. F., Fisher, L. W., Li, K., LeBaron, R. G., Tan, E. M. and Uitto, J. (1995). Differential expression of the versican and decorin genes in photoaged and sun-protected skin. Comparison by immunohistochemical and northern analyses. *Lab. Invest.* **72**, 662-669.

Bi, X., Corpina, R. A. and Goldberg, J. (2002). Structure of the Sec23/24-Sar1 pre-budding complex of the COPII vesicle coat. *Nature* **419**, 271-277.

Bi, X., Mancias, J. D. and Goldberg, J. (2007). Insights into COPII Coat Nucleation from the Structure of Sec23*Sar1 Complexed with the Active Fragment of Sec31. *Dev. Cell* **13**, 635-645.

Bielli, A., Haney, C. J., Gabreski, G., Watkins, S. C., Bannykh, S. I. and Aridor, M. (2005). Regulation of Sar1 NH2 terminus by GTP binding and hydrolysis promotes membrane deformation to control COPII vesicle fission. *J. Cell Biol.* **171**, 919-924.

Boyadjiev, S. A., Justice, C. M., Eyaid, W., McKusick, V. A., Lachman, R. S., Chowdry, A. B., Jabak, M., Zwaan, J., Wilson, A. F. and Jabs, E. W. (2003). A novel dysmorphic syndrome with open calvarial sutures and sutural cataracts maps to chromosome 14q13-q21. *Hum. Genet.* **113**, 1-9.

Boyadjiev, S. A., Fromme, J. C., Ben, J., Chong, S. S., Nauta, C., Hur, D. J., Zhang, G., Hamamoto, S., Schekman, R., Ravazzola, M. et al. (2006). Cranio-lenticulo-sutural dysplasia is caused by a SEC23A mutation leading to abnormal endoplasmic-reticulum-to-Golgi trafficking. *Nat. Genet.* **38**, 1192-1197.

Elrod-Erickson, M. J. and Kaiser, C. A. (1996). Genes that control the fidelity of endoplasmic reticulum to Golgi transport identified as suppressors of vesicle budding mutations. *Mol. Biol. Cell* **7**, 1043-1058.

Fatal, N., Suntio, T. and Makarow, M. (2002). Selective protein exit from yeast endoplasmic reticulum in absence of functional COPII coat component Sec13p. *Mol. Biol. Cell* **13**, 4130-4140.

Fath, S., Mancias, J. D., Bi, X. and Goldberg, J. (2007). Structure and organization of coat proteins in the COPII cage. *Cell* **129**, 1325-1336.

Fisher, L. W., Lindner, W., Young, M. F. and Termine, J. D. (1989). Synthetic peptide antisera: their production and use in the cloning of matrix proteins. *Connect. Tissue Res.* **21**, 43-48; discussion 49-50.

Fromme, J. C., Ravazzola, M., Hamamoto, S., Al-Balwi, M., Eyaid, W., Boyadjiev, S. A., Cosson, P., Schekman, R. and Orci, L. (2007). The genetic basis of a craniofacial disease provides insight into COPII coat assembly. *Dev. Cell* **13**, 623-634.

Futai, E., Hamamoto, S., Orci, L. and Schekman, R. (2004). GTP/GDP exchange by Sec12p enables COPII vesicle bud formation on synthetic liposomes. *EMBO J.* **23**, 4146-4155.

Gallione, C. J. and Rose, J. K. (1985). A single amino acid substitution in a hydrophobic domain causes temperature-sensitive cell-surface transport of a mutant viral glycoprotein. *J. Virol.* **54**, 374-382.

Keller, P., Toomre, D., Diaz, E., White, J. and Simons, K. (2001). Multicolour imaging of post-Golgi sorting and trafficking in live cells. *Nat. Cell Biol.* **3**, 140-149.

Lang, M. R., Lapierre, L. A., Frotscher, M., Goldenring, J. R. and Knapik, E. W. (2006). Secretory COPII coat component Sec23a is essential for craniofacial chondrocyte maturation. *Nat. Genet.* **38**, 1198-1203.

Lee, M. C., Orci, L., Hamamoto, S., Futai, E., Ravazzola, M. and Schekman, R. (2005). Sar1p N-terminal helix initiates membrane curvature and completes the fission of a COPII vesicle. *Cell* **122**, 605-617.

Mancias, J. D. and Goldberg, J. (2005). Exiting the endoplasmic reticulum. *Traffic* **6**, 278-285.

Matsuoka, K., Orci, L., Amherdt, M., Bednarek, S. Y., Hamamoto, S., Schekman, R. and Yeung, T. (1998). COPII-coated vesicle formation reconstituted with purified coat proteins and chemically defined liposomes. *Cell* **93**, 263-275.

McDonald, K., Morphew, M., Verkade, P. and Müller-Reichert, T. (2007). Recent advances in high pressure freezing: equipment and specimen loading methods. In *Methods in Molecular Biology, vol.* **369***, Electron microscopy: methods and protocols* (ed. J. Kuo), pp. 143-173. Totowa, NJ.: Humana Press.

Neuhauss, S. C., Solnica-Krezel, L., Schier, A. F., Zwartkruis, F., Stemple, D. L., Malicki, J., Abdelilah, S., Stainier, D. Y. and Driever, W. (1996). Mutations affecting craniofacial development in zebrafish. *Development* **123**, 357-367.

Pryer, N. K., Salama, N. R., Schekman, R. and Kaiser, C. A. (1993). Cytosolic Sec13p complex is required for vesicle formation from the endoplasmic reticulum in vitro. *J. Cell Biol.* **120**, 865-875.

Salama, N. R., Yeung, T. and Schekman, R. W. (1993). The Sec13p complex and reconstitution of vesicle budding from the ER with purified cytosolic proteins. *EMBO J.* **12**, 4073-4082.

Salama, N. R., Chuang, J. S. and Schekman, R. W. (1997). Sec31 encodes an essential component of the COPII coat required for transport vesicle budding from the endoplasmic reticulum. *Mol. Biol. Cell* **8**, 205-217.

Sato, K. and Nakano, A. (2004). Reconstitution of coat protein complex II (COPII) vesicle formation from cargo-reconstituted proteoliposomes reveals the potential role of GTP hydrolysis by Sar1p in protein sorting. *J. Biol. Chem.* **279**, 1330-1335.

Sato, K. and Nakano, A. (2005). Dissection of COPII subunit-cargo assembly and disassembly kinetics during Sar1p-GTP hydrolysis. *Nat. Struct. Mol. Biol.* **12**, 167-174.

Scales, S. J., Pepperkok, R. and Kreis, T. E. (1997). Visualization of ER-to-Golgi transport in living cells reveals a sequential mode of action for COPII and COPI. *Cell* **90**, 1137-1148.

Stagg, S. M., Gurkan, C., Fowler, D. M., LaPointe, P., Foss, T. R., Potter, C. S., Carragher, B. and Balch, W. E. (2006). Structure of the Sec13/31 COPII coat cage. *Nature* **439**, 234-238.

Stankewich, M. C., Stabach, P. R. and Morrow, J. S. (2006). Human Sec31B: a family of new mammalian orthologues of yeast Sec31p that associate with the COPII coat. *J. Cell Sci.* **119**, 958-969.

Stephens, D. J. (2003). De novo formation, fusion and fission of mammalian COPII-coated endoplasmic reticulum exit sites. *EMBO Rep.* **4**, 210-217.

Stephens, D. J. and Pepperkok, R. (2004). Differential effects of a GTP-restricted mutant of Sar1p on segregation of cargo during export from the endoplasmic reticulum. *J. Cell Sci.* **117**, 3635-3644.

Tang, B. L., Peter, F., Krijnse-Locker, J., Low, S. H., Griffiths, G. and Hong, W. (1997). The mammalian homolog of yeast Sec13p is enriched in the intermediate compartment and is essential for protein transport from the endoplasmic reticulum to the Golgi apparatus. *Mol. Cell. Biol.* **17**, 256-266.

Tang, B. L., Zhang, T., Low, D. Y., Wong, E. T., Horstmann, H. and Hong, W. (2000). Mammalian homologues of yeast sec31p. An ubiquitously expressed form is localized to endoplasmic reticulum (ER) exit sites and is essential for ER-Golgi transport. *J. Biol. Chem.* **275**, 13597-13604.

Thisse, B., Pflumio, S., Fürthauer, M., Loppin, B., Heyer, V., Degrave, A., Woehl, R., Lux, A., Steffan, T., Charbonnier, X. Q. et al. (2001). Expression of the zebrafish genome during embryogenesis (NIH R01 RR15402) (http://zfin.org).

Verkade, P. (2008). Moving EM: the rapid transfer system as a new tool for correlative light and electron microscopy and high throughput for high-pressure freezing. *J. Microsc.* **230**, 317-328.

Walsh, E. C. and Stainier, D. Y. (2001). UDP-glucose dehydrogenase required for cardiac valve formation in zebrafish. *Science* **293**, 1670-1673.

Watson, P. and Stephens, D. J. (2005). ER-to-Golgi transport: form and formation of vesicular and tubular carriers. *Biochim. Biophys. Acta* **1744**, 304-315.

Watson, P. and Stephens, D. J. (2006). Microtubule plus-end loading of p150(Glued) is mediated by EB1 and CLIP-170 but is not required for intracellular membrane traffic in mammalian cells. *J. Cell Sci.* **119**, 2758-2767.

Watson, P., Townley, A. K., Koka, P., Palmer, K. J. and Stephens, D. J. (2006). Sec16 defines endoplasmic reticulum exit sites and is required for secretory cargo export in mammalian cells. *Traffic* **7**, 1678-1687.

Westerfield, M. (1995). *The Zebrafish Book: A Guide For The Laboratory Use Of Zebrafish (Brachydanio Rerio)*. Eugene, OR: University of Oregon Press.